Available online at www.sciencedirect.com
ScienceDirect
Cement and Concrete Research 37 (2007) 902–908
Cement and Concrete Research

# NMR studies of pore formation and water diffusion in self-hardening cut-off wall materials

Wiete Schönfelder [a], Jörg Dietrich [b], Andreas Märten [b], Klaas Kopinga [c], Frank Stallmach [a,*]

[a] Fakultät für Physik und Geowissenschaften, Universität Leipzig, Linnèstraße 5, 04103 Leipzig, Germany
[b] AZBUT Anneliese Baustoffe für Umwelt und Tiefbau GmbH & Co. KG, Neubeckumer Straße 92, 59320 Ennigerloh, Germany
[c] Department of Applied Physics, Eindhoven University of Technology, P.O. Box 513, 5600 MB Eindhoven, The Netherlands

**Abstract**

Cut-off walls for the containment of polluted sites are vertical in-ground barriers of low hydraulic conductivity. To construct these barriers, self-hardening watery suspensions of a special cement-based hydraulic binder and a cement-stable bentonite are used. The formation of the pore structure during hardening of suspensions with different solid contents and the water self-diffusion in the resulting cut-off wall materials were studied by non-destructive $^{1}$H NMR techniques. It was found that an increased amount of hydrating solids in the suspension leads to a decrease in NMR relaxation times and self-diffusion coefficients of the pore water, indicating a reduction of the pore sizes and an enhancement of the diffusion resistance. The self-diffusion coefficients of the water in the hardened cut-off wall materials were determined to be about four orders of magnitude smaller than in bulk liquid water and two orders of magnitude smaller than in pure bentonite–water suspensions confirming the excellent diffusive resistance of the cut-off wall materials.


*Keywords:* Pore size distribution (B); Diffusion (C); Grinded blast-furnace slag (D); Waste management (E); NMR

## 1. Introduction

In the past years, NMR has provided new possibilities of studying building material in a non-destructive way. Cements [1,2], bricks [3,4] and clays [5,6] are examples for materials, in which pore structures, time dependent changes of the content and mobility of water and influences of pollutants have been investigated by NMR relaxometry, diffusometry and cryoporometry, respectively. A totally new field of interest for NMR studies of construction materials are self-hardening cut-off wall materials. These materials are commonly used to build vertical in-ground barriers for the encapsulation of polluted sites and of old uncontrolled waste landfills [7]. In order to construct these vertical barriers a trench, surrounding the polluted site is excavated. To prevent this trench from collapsing, it is filled with the suspension received by mixing the dry and powdery cut-off wall material with water. The suspension is left in the trench, and at the end of the processing time the original liquid-like mixture hardens to a dense and homogeneous wall in subsurface.

The main components of self-hardening cut-off wall materials are a special hydraulic binder, which is rich in grinded blast furnace slag, and a cement-stable bentonite. While excavating the trench, the bentonite-content is important to build up a filter cake, which makes it possible to transmit the hydraulic pressure of the suspension to the trench-walls and therefore to stabilize the trench [8]. The bentonite is also needed to keep the binder particles in abeyance and to ensure low hydraulic permeability after hardening. Due to the slow hydration of the hydraulic binder, the processing time of the cut-off wall suspension is about 8 h, which allows a single-phase operation of trench excavation.

In case of an encapsulation of polluted sites, the cut-off wall material must have a sufficient resistance against the contaminants contained in groundwater and leachate [9]. Furthermore the cut-off wall material must harden properly, even if the soil in situ contains organic substances, which cause a retardation of the

* Corresponding author. Fax: +49 341 973 2549.
*E-mail address:* stallmac@physik.uni-leipzig.de (F. Stallmach).

0008-8846/$ - see front matter © 2007 Elsevier Ltd. All rights reserved.

hydration process. Therefore, the composition of the cut-off wall material has to be adjusted to these local conditions and the suitability of the chosen composition has to be proven by laboratory testing [10]. Up to now, a lot of effort has been made to create materials of low hydraulic conductivity ($<1\times10^{-10}$ ms$^{-1}$) [11], disabling pollutants from penetrating the cut-off wall by dispersion with the water phase. However, time consuming tracer experiments have shown that pollutants might still advance via diffusion [12]. Until now, the influence of ingredients and the content of solids on the microscopic properties of the cut-off wall, like pore structure or diffusivity, is only poorly understood.

To enlarge the knowledge on this specific area, we present for the first time NMR studies on self-hardening cut-off wall materials. $^1$H NMR relaxation times are investigated during hardening (hydration) of such materials in order to obtain information on pore structure parameters in dependence on material composition. These studies are accompanied by pulsed field gradient (PFG) NMR measurements allowing direct assessment of water self-diffusion in the cut-off wall materials.

## 2. Materials and methods

### 2.1. Sample preparation

To produce the samples for NMR relaxation and water self-diffusion measurements, typical powdery ready-made mixes suitable for the production of the watery cut-off wall suspensions with a solid-content of 230, 400 and 600 kg/m$^3$ were obtained from AZBUT (Germany). All mixes contained a special hydraulic binder rich in grinded blast furnace slag and a cement-stable sodium bentonite. One mixture (IIIf, solid content: 600 kg/m$^3$) contained a higher amount of non-hydrating filler material (powdery marl with a $CaCO_3$-content of approx. 66%) that partially replaced the binder-fraction.

The powdery cut-off wall material was mixed with tap water according to its content of solids in a ratio of 1:4, 1:2 and 1:1.3 (see Table 1). These high water contents ensure the initial low viscosities of the cut-off wall suspensions, which are necessary for the simultaneous trench excavation and trench filling. After stirring the suspensions with an electrical mixer for about 3 min, the suspensions were filled in sets of NMR sample tubes. For the low-field NMR relaxometry and cryoporometry studies, glass tubes of 20 mm outer diameter were used. For the PFG NMR diffusometry, the suspensions were filled in glass tubes of 7.5 mm outer diameter. In order to prevent evaporation of water from the suspensions and the hardened cut-off wall materials, all sample tubes were sealed tightly by a cap. The samples were stored at room temperature until the start of the NMR measurements.

Table 1
Solid content and water/solid ratio of the watery suspensions of cut-off wall materials for NMR relaxation and diffusion studies

| Sample | Solid content, kg/m$^3$ | Water/solid, g/g |
|---|---|---|
| I | 230 | 4.0 |
| II | 400 | 2.15 |
| III | 600 | 1.3 |
| IIIf[a] | 600 | 1.3 |

[a] Same total solid content as sample III but fraction of hydraulic binder replaced by non-hydrating filler.

### 2.2. Low-field NMR relaxometry

To study pore structures and hardening processes, the decay of the transverse magnetization ($T_2$) of the $^1$H nuclei of the water phase was measured using the CPMG NMR pulse sequence [13,14]. After the initial exciting $\pi/2$ rf pulse, 1024 spin echoes were generated by successive $\pi$ rf pulses. The inter echo time was set to $\tau=100$ μs. The studies were performed with a low-field NMR spectrometer operating at 9.1 MHz $^1$H resonance frequency. It is equipped with a PC controlled MARAN DRX console (Resonance Instruments, GB) and a home-built sensor system consisting of two opposing NdFeB permanent magnets, which generate a magnetic flux density of 0.21 T for the polarizing magnetic field, and a solenoid rf-coil suitable for NMR sample tubes of 20 mm outer diameter (for details see Ref. [1]).

These CPMG NMR measurements were performed on three samples of each composition. Due to the high water content of the cut-off wall material, it was sufficient to add up 64 scans to obtain a good signal-to-noise ratio. The repetition time was varied from 15 s for the liquid-like suspension to 5 s for the hardened material. All relaxation time measurements were performed at 22 °C. Assuming that the total magnetization decay is given by a superposition of exponential decays, the distributions of $T_2$ were calculated by a regularized inverse Laplace transformation using WINDXP software (Resonance Instruments, GB). These $T_2$ distributions yield information about the total signal intensity (area under the distribution), which is directly proportional to the physically bound water. The $T_2$ relaxation times and their logarithmic mean value $\langle T_2\rangle$ may be interpreted in terms of the pore size $R$ of the material using the relation [15]

$$\frac{1}{T_2}=\rho\cdot\frac{1}{R}, \tag{1}$$

where $\rho$ denotes the surface-relaxivity parameter. Since $\rho$ depends on the chemical composition of the pore-matrix interface, absolute determinations of pore sizes based on CPMG NMR and Eq. (1) are difficult and represent often just a rough estimate. However, since the cut-off wall suspensions and the hardened cut-off wall materials consist of the same raw materials, a qualitative interpretation of the acquired relaxation time distribution data in terms of changes in pore size for the different mixtures and for each mixture during hardening is justified.

### 2.3. NMR cryoporometry

The accurate determination of pore sizes of the hardened cut-off wall material is a difficult task, because the removal of water as required by many methods leads to a structural breakdown of

the samples. An ideal way to get information about the mean size of the pores filled with water provides the application of NMR cryoporometry. This method utilizes the melting point depression in small pores and the fast (non-observable) relaxation of frozen water ($T_2 \sim 6$ μs) [16]. To avoid supercooling of the pore water during the cryoporometry studies, the samples of the hardened cut-off wall materials were first cooled down to 225 K, where no NMR signal could be observed in the CPMG experiment since all pore water is frozen. Successively, CPMG NMR measurements were performed at increasing temperatures. The sample temperature was determined from the resistance of a miniature Pt100 thermometer, located at the side of the sample. Because of the linear correlation between the melting point depression and the reciprocal pore size [17], the steepest increase in signal intensity can be interpreted in terms of the dominant pore radius $a$. Using the Gibbs–Thomson relation [18,19], one obtains for the melting point depression $\Delta T_m$

$$\Delta T_m = T_m(a) - T_m(\infty) = \frac{k}{a}, \tag{2}$$

where $T_m(\infty)$ is the bulk melting temperature and $k$ a parameter depending on properties of the confined liquid. For water, which is the pore fluid in this study, a value of $k = 8.5 \times 10^{-8}$ Km as suggested in [20] was chosen for the interpretation of the NMR cryoporometry. The measurements were performed on two hardened samples (230 kg/m$^3$ and 600 kg/m$^3$) of a diameter of 20 mm in a field of magnetic flux density of 0.8 T, corresponding to a $^1$H resonance frequency of 31 MHz.

### 2.4. NMR diffusometry

PFG NMR self-diffusion studies were performed on hardened samples of the cut-off wall material (Table 1) roughly 1 month after sample preparation using our home-built NMR spectrometer FEGRIS NT operating at a $^1$H resonance frequency of 125 MHz [21]. The self-diffusion coefficients of the pore water $D_{eff}$ were obtained by measuring the attenuation of the NMR spin echo signal as a function of the amplitude of the pulsed field gradients. Due to the $\tau$ independent $T_2$ relaxation decays observed in CPMG NMR experiments at this resonance frequency, we concluded that disturbing influences of internal field gradients are negligible for these samples. Therefore, the stimulated spin echo sequence [22] was applied, for which the spin echo attenuation is given by

$$\Psi = \exp\left\{-(\gamma g \delta)^2 D_{eff}\left(t - \frac{1}{3}\delta\right)\right\}. \tag{3}$$

In Eq. (3), $g$ and $\delta$ denote the amplitude and width of the pulsed field gradients, respectively, and $\gamma$ represents the gyromagnetic ratio ($\gamma = 2.67 \times 10^8$ (Ts)$^{-1}$ for $^1$H nuclei). The time scale over which the diffusion process is monitored is given by the separation $t$ of the two pulsed field gradients in the pulse sequence. In order to get information on the microscopic structure of the material, the observation time $t$ was varied in a range of 10 ms up to 240 ms. Pulsed field gradient amplitudes $g$ of up to 30 T/m were necessary in order to obtain significant spin echo attenuations. The time-dependent effective self-diffusion coefficients obtained via Eq. (3) from the measured spin echo attenuations were used to calculate the time dependence of the mean square (r.m.s.) displacements of the water molecules using the Einstein relation

$$\langle r^2(t) \rangle = 6 D_{eff} t. \tag{4}$$

## 3. Results and discussion

### 3.1. Relaxation studies on hardening cut-off wall material

Changes of the transverse relaxation time $T_2$ and NMR signal intensity in the hardening cut-off wall material were monitored by low-field CPMG NMR during the first 4 days after sample preparation. Already 1 h after sample preparation (Fig. 1), when the mixture is still a low-viscous suspension, it is easy to distinguish between the mixes of different content of solids by the peak positions in the distribution of $T_2$ and the difference in signal intensity (area under the $T_2$ distribution). Sample I (230 kg/m$^3$) shows the largest area, which is reasonable since it is the mixture with the highest water content (see Table 1). With increasing content of solids and, therefore, decreasing water content, the NMR signal intensity decreases, as expected, and the relaxation time distribution shifts towards shorter times. This behavior is due to the larger quantity of solid particles. The water molecules interact with the surface of solids where – depending to the surface relaxivity – they lose their contribution to the total NMR signal with a certain probability and, thus, reduce the observed $T_2$ relaxation time.

Starting roughly 1 day after sample preparation, we observe a shift of the relaxation time distributions to the left (Fig. 2a), while the shape of the distributions obtained from the individual

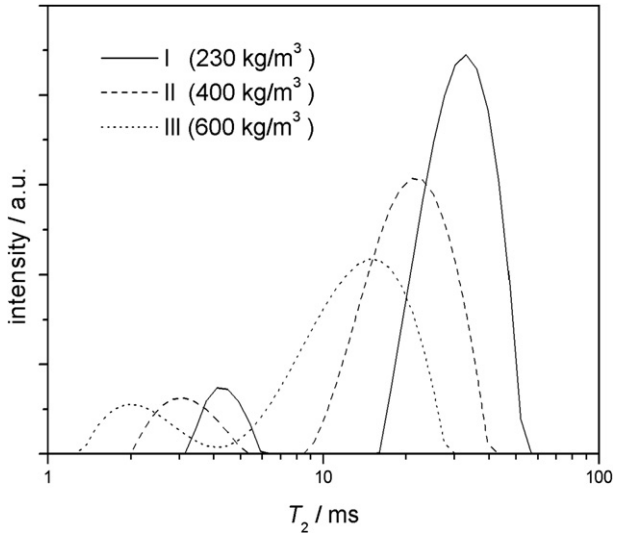


Fig. 1. Distribution of transverse relaxation times $T_2$ of freshly mixed cut-off wall suspensions of different solid content.

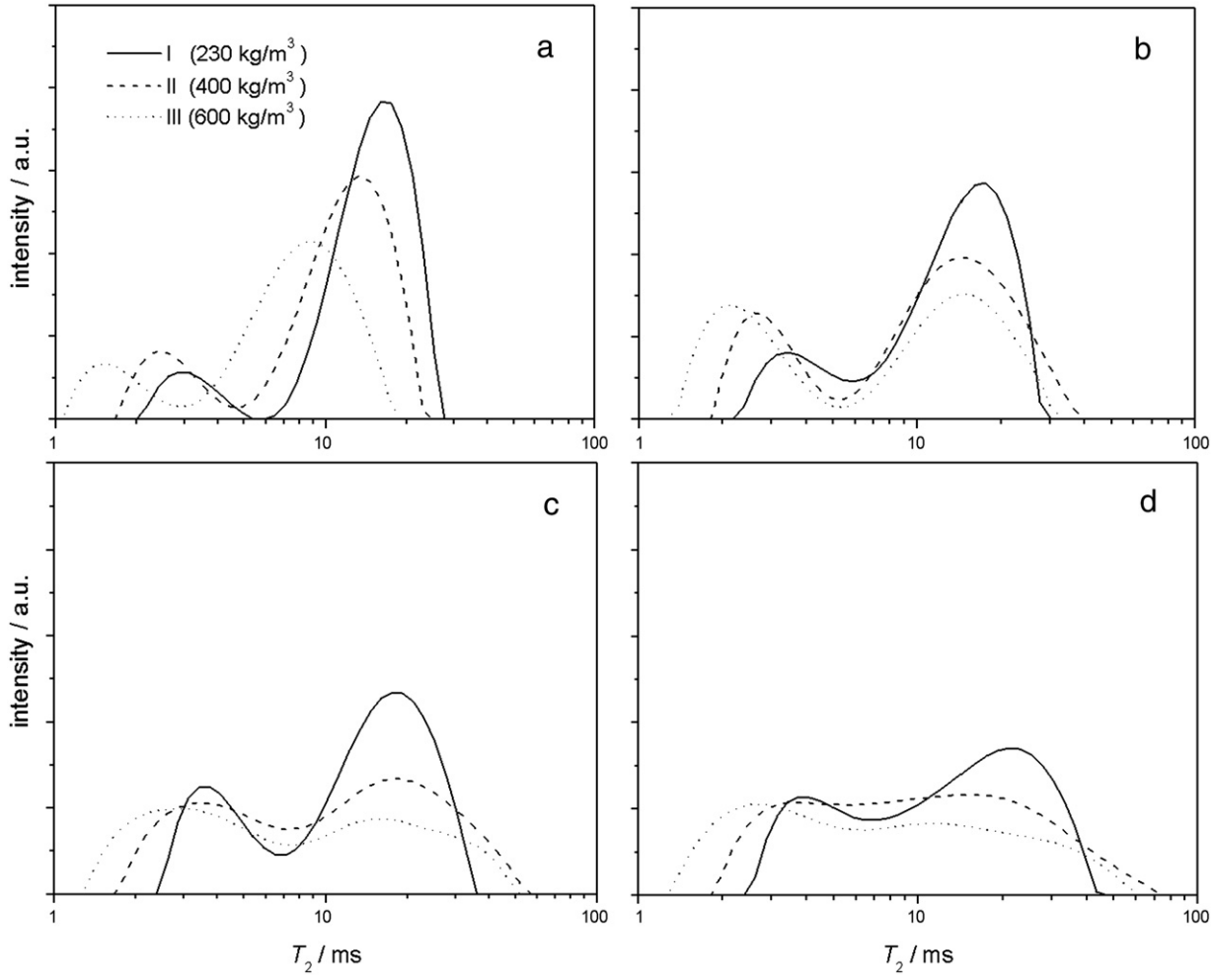


Fig. 2. Distributions of transverse relaxation times $T_2$ of hardening cut-off wall materials of different solid content 24 h (a), 48 h (b), 72 h (c) and 96 h (d) after sample preparation.

mixtures with different contents of solids is still not changing significantly compared to the shape of the distribution of the freshly mixed suspensions (Fig. 1). The observed decrease in logarithmic mean relaxation time, which is associated with the left-shift of the relaxation time distribution, may be interpreted as a decrease of mean pore sizes. The reason for this decrease in pore size is the onset of the hydration of the hydraulic binder. The hydration products like the spicular calcium–silicate–hydrates (CSH) growing on the surface of the binder particles bridge the inter-particle spaces, which leads to the stiffing of the mix starting approximately 10 h after preparation [23]. Due to the ongoing growth of hydrate crystals, the size of the water filled pores is reduced. The changes in the $T_2$ relaxation time distributions observed during the first 4 days after sample preparation (Fig. 2a–d) show that NMR signal intensity from water in large pores, which appears at long $T_2$ relaxation times, decreases and the intensity from water in smaller pores (short relaxation times) increases with ongoing hydration. The relaxation time distributions obtained 3 and 4 days after sample preparation (Fig. 2c,d) show that the process of hydration leads to a homogenization of the pore size distribution: The initial high amount of large pores and of large particle–particle distances in the fresh cut-off wall suspension, respectively, is diminished. This increases the amount of small pores (peaks at short $T_2$ relaxation times) and reduces at the same time the mean pore radius and, consequently, the logarithmic mean relaxation time.

By analyzing the area under the $T_2$ relaxation time distributions plotted in Figs. 1 and 2, one finds a continuous slight decrease in NMR signal intensities for each sample. Four days after sample preparation (Fig. 2d), it does not exceed 10% of the initially observed signal intensity (Fig. 1). As shown in an earlier study on hydrating cement pastes [1], this loss in NMR signal is caused by the consumption of pore water by the hydration reaction. Since the experimental condition chosen for these low-field CPMG NMR studies do not allow to observe an NMR signal from the chemically bound $^1$H nuclei of the solid hydrate crystals formed during hydration, the remaining 90% of the initial NMR signal must originate from water, which is physically bound in the pore space between the solids of the cut-off wall material. The high amounts of physically bound water after the initial hardening period correspond to mass fractions ($m_{f,\mathrm{H2O}}$) of about 0.8 to 0.5 gram water per gram of the hardened cut-off wall material (see Table 2 for details). These are rather

Table 2
NMR determined properties of cut-off wall samples: logarithmic mean relaxation time 1 h ($\langle T_2\rangle^a$) and 3 weeks ($\langle T_2\rangle^b$) after sample preparation; content of physically bound pore water ($m_{f,H2O}$), mean pore radius $a$, and characteristic exponent $\kappa$ of the time dependence of the effective diffusivity $D_{eff}$ of the hardened cut-off wall samples

| Sample | $\langle T_2\rangle^a$, ms | $\langle T_2\rangle^b$, ms | $m_{f,H2O}$, g/g | $a$, μm | $D_{eff}$, $m^2\ s^{-1}$ | $\kappa$ |
|---|---|---|---|---|---|---|
| I | 19.0 | 14.4 | 0.73 | 0.14 | $2.2\times10^{-13}$ | 0.71 |
| II | 18.0 | 10.9 | 0.66 | – | $1.7\times10^{-13}$ | 0.70 |
| III | 12.2 | 9.3 | 0.54 | 0.05 | $0.9\times10^{-13}$ | 0.48 |
| IIIf | 15.1 | 13.6 | 0.54 | – | $1.3\times10^{-13}$ | 0.70 |

high water contents for materials, which are developed to prevent transport of pollutants. Nevertheless, as we will show below, the small size of the pores and the homogenous pore size distribution are the main reason for the excellent diffusion resistance of the self-hardening cut-off wall materials.

### 3.2. Relaxation studies on hardened cut-off wall material

Three weeks after sample preparation, the hydration of the blast furnace slag in the hydraulic binder is still in progress [24]. It led to a further reduction of the amount of large pores, which is shown in the relaxation time distribution presented in Fig. 3 by the smaller intensities at long $T_2$ relaxation times compared to Fig. 2d. Additionally, clear differences between the relaxation time distributions of the mixes of different solid content are observed (Fig. 3). The logarithmic mean transverse relaxation time $\langle T_2\rangle$ is decreasing with increasing content of solids in the cut-off wall material (Table 2). This behavior results, as discussed above, from the dependence of the pores size on the initial solid content. A higher content of hydrating solids induces the closure of pores and reduction of pore size, resulting in faster relaxation and less signal intensity. Thus, the increased formation of smaller pores explains the reduction of relaxation times observed in mixtures with an increased content of solid ingredients, as e.g. sample III (Fig. 3).

Compared to sample III, sample IIIf, which contains a certain fraction of non-hydrating filler, shows a distinct bimodal relaxation time distribution and a longer logarithmic mean relaxation time (Fig. 3 and Table 2). This observation evidences that the presence of non-reacting grains of the filler leads to larger water-saturated vacant spaces in the pore space adjoined to these grains. We assume that hydration products, which increasingly fill up the pore spaces during hydration, mainly develop on the surface of binder grains. Therefore, a clear distinction occurs between the observed relaxation time distributions and, thus, the pore sizes of sample III (no filler) and IIIf (with filler) although both samples contain the same total amount of solids.

### 3.3. Determination of mean pore sizes by cryoporometry

To obtain quantitative information about the mean pore size of the hardened cut-off wall material, the melting point depression of water within the sample of the lowest (sample I, 230 kg/m$^3$) and highest (sample III, 600 kg/m$^3$) content of solids was determined by cryoporometry. Fig. 4 shows the total NMR signal intensity measured at increasing temperatures. The lowest temperatures, for which NMR signals from liquid (molten) pore water could be observed, are about 250 K for sample III and 258 K for sample I. According to Eq. (2), these temperatures correspond to pore radii of about 4 nm in sample III and about 6 nm in sample I. These values represent the minimum pore radii of these two samples. They are consistent with the relaxation time distributions plotted in Fig. 3, where the observed shortest relaxation time components shift from about 5 ms in sample I to about 3 ms in sample III. Additionally, the mean melting point depressions of these samples were found to be about (1.7±0.2) K for sample III and about (0.6±0.1) K for sample I. According to Eq. (2), this corresponds to a mean pore radius of $a=(0.14\pm0.02)$ μm for sample I and $a=(0.05\pm0.01)$ μm for sample III. Table 2 shows that the logarithmic mean relaxation time $\langle T_2\rangle$ of the relaxation time distribution and the mean pore radius $a$ determined by NMR cryoporometry evidence the same trend in pore size characteristics of these samples: An increasing amount of hydrating solids leads to smaller pores in the hardened cut-off wall materials.

### 3.4. Diffusion studies by PFG NMR

The dependence of the mean pore size on the content of solids in the cut-off wall material is directly reflected in the results of PFG NMR diffusion studies. The self-diffusion coefficients of water in the mixtures measured at different observation times 1 month after preparation are plotted in Fig. 5. They are more than two orders of magnitude smaller than water diffusion in pure bentonite suspensions [25,26]. The diffusion coefficients decrease with increasing content of solids. However, sample IIIf, in which a fraction of the hydraulic binder was replaced by non-hydrating filler, is characterized by higher self-diffusion coefficients than the sample of original

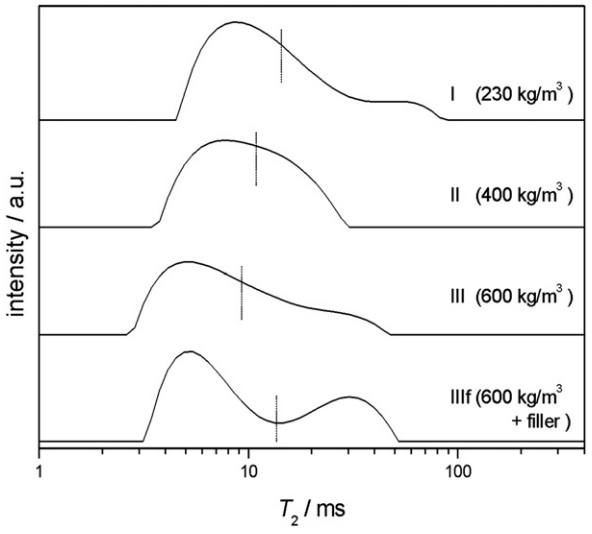


Fig. 3. Distribution of transverse relaxation time $T_2$ of the hardened cut-off wall materials of different solid content 21 days after sample preparation. Dotted lines indicate the logarithmic mean $T_2$ values given in Table 2.

composition (sample III). This agrees well with the longer mean relaxation times observed by relaxometry, proving the assumption that the addition of non-hydrating filler leads to an increased pore size.

In contrast to clay gels, where the self-diffusion coefficients were found to be independent on observation time [25], the hydration induced solid structure of the cut-off wall is restricting the self-diffusion. The experimentally observed dependence of the diffusion coefficient $D_{\mathrm{eff}}$ on the observation time $t$ can be described empirically by a power law

$$D_{\mathrm{eff}}(t) \propto t^{\kappa-1}, \tag{5}$$

where $\kappa$ denotes an empirical exponent. Whereas for unrestricted normal diffusion, the empirical exponent is expected to be equal to unity, which corresponds to a time-independent effective self-diffusion coefficient, $\kappa<1$ indicates anomalous restricted diffusion [27], where the diffusivity decreases with increasing observation time. In the limiting case of completely restricted diffusion as, e.g., in closed pores, which are not interconnected, one has $\kappa=0$ corresponding to $D_{\mathrm{eff}}$ being proportional to $t^{-1}$. For the water self-diffusion in the cut-off wall materials, we found $0.5<\kappa<0.8$ (Table 2), corresponding to the case of anomalous but not completely restricted diffusion. Fig. 5 shows that the strongest time dependence of the water self-diffusion, which is associated with the smallest value of $\kappa$ in Table 2 and, thus, the best approximation to the case of closed pores, was observed for the material with the highest content of solids and hydraulic binder (sample III). Replacing the hydraulic binder by a non-hydrating filler (sample IIIf) leads to higher self-diffusion coefficients and a significantly larger $\kappa$ value, both indicating a less effective diffusional resistance of the solid pore matrix of the hardened cut-off wall material.

The maximal root mean square (r.m.s.) displacements of the water in the cut-off wall materials observed by the PFG NMR technique are approximately 0.4 μm (sample I at 240 ms diffusion time, compare Fig. 5). This value corresponds roughly

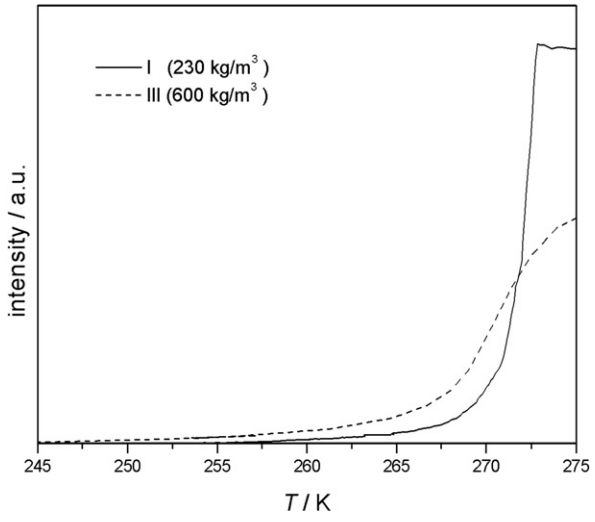


Fig. 4. Increase in NMR signal intensity with increasing sample temperature observed by NMR cryoporometry.

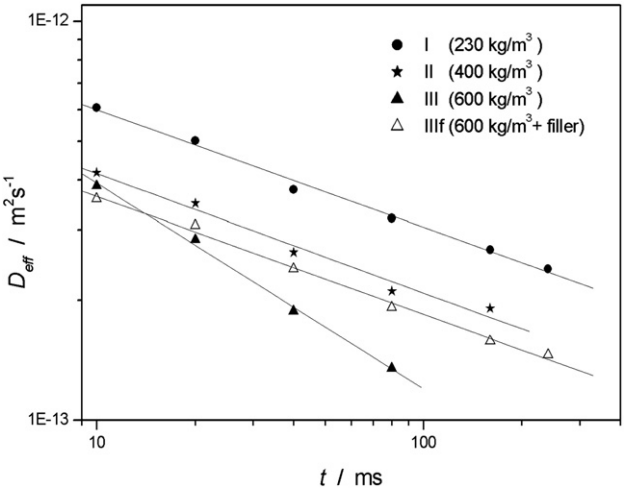


Fig. 5. Effective diffusion coefficient of the physically bound pore water as a function of the observation time $t$ for the hardened cut-off wall materials (1 month old) with different content of solids (I, II, III, IIIf). The lines in this log–log presentation were obtained by a exponential fit yielding the exponent $\kappa$ defined in Eq. (5).

to three times the pore diameter. Thus, the pore space of the hardened cut-off wall material is interconnected on the small length scale of the NMR diffusion studies. However, already at the shortest accessible diffusion times (10 ms), the interaction of the physically bound pore water with clay and hydrated binder reduces the water diffusion by more than three orders of magnitude compared to bulk liquid water. At a diffusion length scale slightly exceeding the pore size measured by NMR cryoporometry, the reduction of pore water diffusivity reaches already four orders of magnitude. These data evidence the excellent diffusional resistance of the hardened cut-off wall materials, which – regardless of the high mass fractions of physically bound water – strongly restrict diffusion processes already on the length scale of the typical pore dimension.

## 4. Conclusion

The results of NMR relaxometry as well as cryoporometry and diffusometry lead to a consistent view of the interconnection between solid content and pore size of the self-hardening cut-off wall material. An increase in content of hydrating solids leads to a decrease in relaxation time and diffusion coefficients, indicating a reduction of pore sizes. A partial replacement of hydrating solids by non-hydrating filler material increases the pore size and simultaneously decreases the diffusional resistance of the resulting cut-off wall. The different pore sizes of the different mixtures were verified by cryoporometry. The water self-diffusion coefficients measured by PFG NMR have been determined to be more than two orders of magnitude lower than estimated from earlier tracer experiments, where a value of $5\times10^{-11}$ $\mathrm{m^2\ s^{-1}}$ was found for a similar material [11]. This might be due to the small volume and homogeneity of our NMR samples as well as the small length scale over which the NMR probes diffusion processes. With the determination of very low diffusion coefficients and the composition dependent trends in

pore size, NMR has proven to be a useful tool to study cut-off wall materials. The application of the different NMR methods described in this paper might help to support and improve the development of new mixtures for self-hardening cut-off walls and may be used to optimize site-specific compositions.

## Acknowledgement

Financial support by the DFG (Germany) and the NWO (The Netherlands) via their joint International Research Training Group "Diffusion in Porous Materials" is gratefully acknowledged.

## References

[1] K. Friedemann, F. Stallmach, J. Kärger, NMR diffusion and relaxation studies during cement hydration — a non-destructive approach for clarification of the mechanism of internal post curing of cementitous materials, Cement and Concrete Research 36 (2006) 817–826.
[2] N. Nestle, A simple semiempiric model for NMR relaxometry data of hydrating cement pastes, Cement and Concrete Research 34 (2004) 447–454.
[3] S. Sharma, F. Casanova, W. Wache, A. Segre, B. Blümich, Analysis of historical porous building materials by the NMR-mouse®, Magnetic Resonance Imaging 21 (2003) 249–255.
[4] J. Petković, H.P. Huinink, L. Pel, K. Kopinga, Diffusion in porous building materials with high internal magnetic field gradients, Journal of Magnetic Resonance 167 (2004) 97–106.
[5] Y. Nakashima, F. Mitsumori, $H_2O$ self-diffusion restricted by clay platelets with immobilized bound $H_2O$ layers: PGSE NMR study of water-rich saponite gels, Applied Clay Science 28 (2005) 209–221.
[6] S. Suzuki, H. Sato, T. Ishidera, N. Fujii, Study on anisotropy of effective diffusion coefficient and activation energy for deuterated water in compacted sodium bentonite, Journal of Contaminant Hydrology 68 (2004) 23–37.
[7] Deutsche Gesellschaft für Geotechnik, GDA-Empfehlungen Geotechnik der Deponien und Altlasten, Ernst & Sohn, Berlin, 1997 (in German).
[8] M. Kilchert, J. Karstedt, Standsicherheitsberechnungen von Schlitzwänden nach DIN 4126, Beuth Verlag, Berlin, 1984 (in German).
[9] R. Wienberg, R. Khorasani, Beständigkeit von Dichtwandmassen für die Altlasteneinkapselung gegen kalklösende Kohlensäure, Altlasten Spektrum, Bd. 4 (1995) 192–198 (in German).
[10] C. Scholz, M. Rosenberg, J. Dietrich, A. Märten, Laborative Eignungsprüfungen von Einphasen-Dichtwandmassen, Geotechnik 1 (2003) 33–41 (in German).
[11] C. Scholz, M. Rosenberg, J. Dietrich, A. Märten, Bestimmung des Durchlässigkeitsbeiwertes an Einphasen-Dichtwandmassen-Untersuchungen zur aktualisierten DIN 18130-1, Bautechnik 80 (2003) 90–97 (in German).
[12] R. Wienberg, Altlasten Spektrum, Bd. 5 (1998) 274–280 (in German).
[13] H.Y. Carr, E.M. Purcell, Effects of diffusion on free precession in NMR experiments, Physical Review 94 (1954) 630–638.
[14] S. Meiboom, D. Gill, Compensation for pulse imperfections in Carr-Purcell NMR experiments, Review of Scientific Instruments 29 (1958) 688–691.
[15] K.R. Brownstein, T.C. Tarr, Importance of classical diffusion in NMR-studies of water in biological cells, Physical Review A 19 (1979) 2446–2453.
[16] K. Overloop, L. van Gerven, Freezing phenomena in adsorbed water as studied by NMR, Journal of Magnetic Resonance. Series A 101 (1993) 179–187.
[17] C.L. Jackson, G.B. McKenna, The melting behavior of organic materials confined in porous solids, Journal of Chemical Physics 93 (1990) 9002–9011.
[18] J.W. Gibbs, Collected Works, New York, 1928.
[19] W. Thomson, On the equilibrium of vapour at a curved surface of liquid, Philosophical Magazine 42 (1871) 448–452.
[20] R. Valckenborg, NMR on technological porous materials, PhD Thesis, Eindhoven, 2001.
[21] P. Galvosas, F. Stallmach, G. Seiffert, J. Kärger, U. Kaess, G. Majer, Generation and application of ultra-high-intensity magnetic filed gradients pulses for NMR spectroscopy, Journal of Magnetic Resonance Spectroscopy 151 (2001) 260–268.
[22] J.E. Tanner, Use of the stimulated echo in NMR diffusion studies, Journal of Chemical Physics 52 (1970) 2523.
[23] M. Geil, Untersuchungen der physikalischen und chemischen Eigenschaften von Bentonit-Zement-Suspensionen im frischen und erhärteten Zustand, PhD Thesis, Braunschweig, 1989 (in German).
[24] J. Stark, B. Wicht, Anorganische Bindemittel, Schriften der Bauhaus-Universität Weimar, vol. 109, 1998 (in German).
[25] Y. Nakashima, Pulsed field gradient proton NMR study of the self-diffusion of $H_2O$ in montmorillonite gel: Effects of temperature and water fraction, American Mineralogist 86 (2001) 132–138.
[26] S. Suzuki, H. Sato, T. Ishidera, N. Fujii, Study on anisotropy of effective diffusion coefficient and activation energy for deuterated water in compacted sodium bentonite, Journal of Contaminant Hydrology 68 (2004) 23–37.
[27] J. Kärger, F. Stallmach, PFG NMR studies of anomalous diffusion, in: P. Heitjans, J. Kärger (Eds.), Diffusion in Condensed Matter, Springer-Verlag, Berlin, 2005, pp. 417–459.